ENVIRONMENTAL RESEARCH
LETTERS

LETTER • OPEN ACCESS

# Invasive *Phragmites* provides superior wave and surge damage protection relative to native plants during storms

To cite this article: Y Peter Sheng *et al* 2021 *Environ. Res. Lett.* **16** 054008

View the article online for updates and enhancements.

This content was downloaded from IP address 65.73.211.90 on 26/07/2021 at 18:25

ENVIRONMENTAL RESEARCH
LETTERS

OPEN ACCESS

RECEIVED
12 November 2020

REVISED
22 February 2021

ACCEPTED FOR PUBLICATION
26 March 2021

PUBLISHED
16 April 2021

Original content from this work may be used under the terms of the Creative Commons Attribution 4.0 licence.

Any further distribution of this work must maintain attribution to the author(s) and the title of the work, journal citation and DOI.

LETTER

# Invasive *Phragmites* provides superior wave and surge damage protection relative to native plants during storms

**Y Peter Sheng*, Adail A Rivera-Nieves, Ruizhi Zou, Vladimir A Paramygin, Christine Angelini and Sean J Sharp**

Engineering School of Sustainable Infrastructure and Environment, University of Florida, Gainesville, FL 32601, United States of America
* Author to whom any correspondence should be addressed.

**E-mail:** pete@coastal.ufl.edu

**Keywords:** Phragmites-dominant Piermont Marsh, Village of Piermont, ecosystem service value of tidal marsh for flood protection, surge and wave, green infrastructure, Natural and Nature-Based Features

Supplementary material for this article is available online

## Abstract

*Phragmites* marshes, which are found in every continent except in Antarctica, are being removed by resource managers in the US because it is considered an invasive species with little ecosystem service value. Here we present a comprehensive study on the ecosystem service value of an invasive *Phragmites* marsh vs a native *Typha* marsh for flood protection during tropical cyclones. Using a vegetation-resolving three-dimensional surge-wave model and observed vegetation and building data, we assessed the value of the Piermont Marsh in buffering Piermont Village, New York, USA from wave, flood, and structural damage during Superstorm Sandy in October 2012. Observed and simulated wind and water level data along the Hudson River were used as boundary conditions. Model results showed that the Marsh, with predominantly invasive *Phragmites australis,* dissipated more than half of the wave energy, but negligible flood, at the Village during Sandy. River-borne debris could not be transported across the Marsh to the Village. If *Phragmites* were replaced with the shorter, native cattail, *Typha angustifolia*, simulations of Sandy suggested that Piermont Marsh's wave and debris buffering capacity would be preserved. However, had Sandy occurred in non-growth season when *Typha* is much shorter and sparser, the Marsh would be unable to buffer the wave and debris. Simulated residential structure damage during Sandy (>$10 M) agreed well with reported losses. If the Marsh were absent, the total loss would have increased by 26%. Since damage is dependent on the storm characteristics, we estimated the protective value of the *Phragmites* marsh for a 1% annual chance flood and wave event to be more than $2 M. This confirms the significant value of Piermont Marsh in protecting Piermont Village from flood and wave damage. To develop a balanced restoration plan, marsh managers should consider biodiversity as well as the significant ecosystem service value of *Phragmites*-dominated marsh for flood protection.

## 1. Introduction

Coastal wetlands are natural and nature-based features which can protect coastal communities from damage due to coastal inundation during storms, high tides, and sea-level rise (SLR). Coastal communities and government resource managers are eager to understand and take advantage of the ecosystem service value of coastal wetlands for flood protection. Recent studies (see e.g. Sheng *et al* 2012, Hu *et al* 2014, Paramygin *et al* 2017, Losada *et al* 2018) showed that tidal marshes and mangroves with adequate stem density and height as well as cross-shore and alongshore widths can buffer storm-induced coastal flooding. During Superstorm Sandy in October 2012, coastal communities in New Jersey (NJ), New York (NY), and Connecticut (CT) experienced significant flooding damage [Federal Emergency Management Agency (FEMA) 2013]. Based on numerical simulation of coastal flooding during Sandy and damage analysis, Narayan *et al* (2017) claimed that coastal marshes and woody wetlands significantly reduced

© 2021 The Author(s). Published by IOP Publishing Ltd

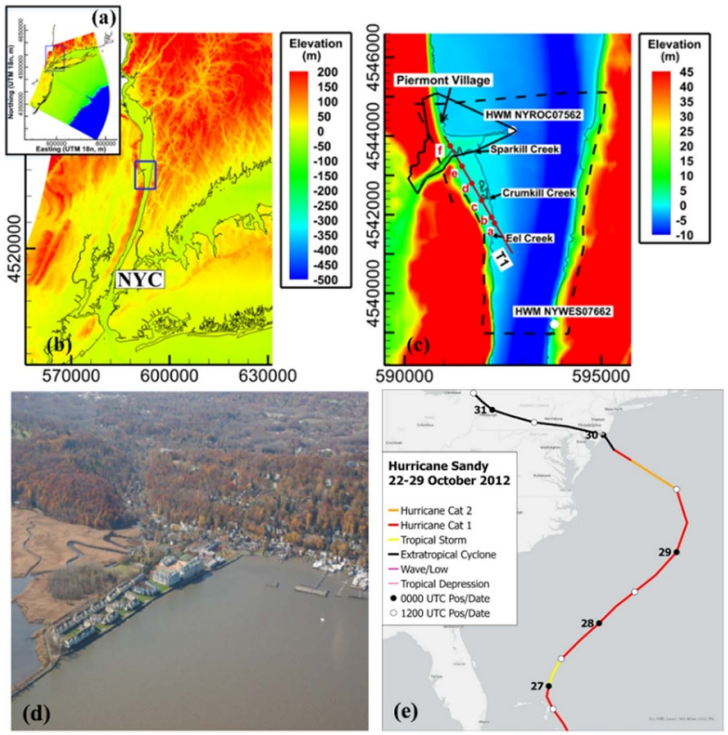


**Figure 1.** (a) Large-scale model domain of this study; (b) lower Hudson River (marked by the blue rectangular in (a)); (c) model domain of Piermont Marsh (enclosed by the black dashed polygon) and Village of Piermont (bounded by the black solid lines); (d) aerial view of Piermont Village and Marsh from the northeast (Photograph credit: Jeff Anzevino/Scenic Hudson. Reproduced with permission); (e) best track of Superstorm Sandy in 2012 (adapted from Blake *et al* (2013). Image stated to be in the public domain).

property damage along the tri-state coasts. Their predictions, however, were not verified against the National Flood Insurance Flood Program (NFIP) loss payout data ($3.9 B for NJ alone) and their model did not incorporate detailed wetland data (plant species, height, and density). Using actual loss and marsh data, Lathrop *et al* (2019) found that the presence of *Spartina* marshes in south NJ had little role in buffering exposed residential structures from storm surge, due to the low (0.3–1 m) marsh height, consistent with the high NFIP payouts there. Sheng *et al* (2021) conducted a comprehensive study on the role of tidal marshes in affecting coastal inundation along NJ/NY/CT coasts during Sandy, a hypothetical extreme Black Swan storm, and the 1% annual chance flood and wave event.

During Sandy, residents in the Piermont Village (figure 1), approximately 15 miles upstream of New York City (NYC) along Hudson River, experienced minor flood damage (with $3.56 M NFIP payout) in comparison to other coastal communities in the tri-state region due to sheltering of the Piermont Marsh to the south. The tall (>2 m) and dense vegetation (>200 stems $m^{-2}$) in the Marsh is predominantly (92%) the non-native invasive common reed, *Phragmites australis*. *Phragmites* grows on all continents except Antarctica and is among the most prolific invasive plants in North American wetlands, including fresh, brackish, and salt marshes located along the Hudson River (Kettenring *et al* 2011). Before the widespread invasion of *Phragmites*, cattail, *Typha angustifolia*, a native species that experience more significant seasonal die-back than *Phragmites* was regionally prevalent in brackish, tidal marshes like Piermont. Due to *Phragmites*' ability to alter biodiversity and ecosystem functions, marsh managers have focused on marsh restoration in *Phragmites*-dominated ecosystems via invasive plant removal which can be very challenging and costly (Kettenring and Adams 2011). On the other hand, numerous studies have found that *Phragmites* marshes do offer valuable ecosystem services by providing habitats to many fish and bird species (Benoit and Askins 1999, Weinstein and Balletto 1999, Weinstein *et al* 2000, Hanson *et al* 2002, Weis and Weis 2003, Weis 2005, Kiviat 2013). *Phragmites* marshes are effective in removal of nutrient (Toyama *et al* 2016) and heavy metal (Windham *et al* 2001), carbon sequestration (Lal 2004), and combating SLR (Rooth and Stevenson 2000, Theuerkauf *et al* 2017). The role and value of *Phragmites* marsh in flood protection, however, is not well understood. While residents of the Piermont Village would like to keep the Piermont Marsh as a barrier to reduce storm-induced flood damage, marsh managers have been considering a potential restoration plan which may include partial *Phragmites* removal. Residents and managers agreed that, prior to developing any restoration plan,

a study is needed to understand the role of Piermont Marsh in protecting residents of Piermont Village from storm-induced flood damage.

The physiological and phenological differences between the two species in this study, *P. australis* and *T. angustifolia*, as well as the positioning of this marsh adjacent to a built community affected by an intense storm event, make Piermont Marsh an ideal study site to investigate the role of marsh vegetation in protecting coastal communities from storm-induced flooding and waves. With abundant vegetation data (plant species, distribution, height, and stem density) as well as other data (water level, wave, and damage) during Sandy, this study used a three-dimensional vegetation-resolving surge-wave model CH3D-SWAN (Sheng *et al* 2012, Sheng and Zou 2017) to quantify the role Piermont Marsh played in buffering residents of the Village of Piermont from massive flood-related damage during Sandy and other potential storms. Value of the Piermont Marsh was assessed by comparing the effects of two vegetation types (*Phragmites, Typha*, and a no vegetation control) on storm surge, wave energy, flood extent, and structural damage during storm events. Following the schematics shown in figure SI 1 (available online at stacks.iop.org/ERL/16/054008/mmedia), this study focuses on the simulation of flood and wave in the high-resolution Piermont region while using results from the large-scale model simulation for the tri-state region (see SI and Sheng *et al* 2021 for description). The surge-wave model CH3D-SWAN and simulation results are described in sections 2–4, while the economic analysis is described in section 5, followed by conclusions in section 6.

## 2. Method

### 2.1. A 3D vegetation-resolving surge-wave model

CH3D-SSMS is an integrated storm surge modeling system, incorporating a coastal surge model CH3D (Sheng 1986, 1989) and a wave model SWAN (Booij *et al* 1999). CH3D and SWAN are dynamically coupled to simulate the time-varying surge and wave fields. Details of the coupling mechanism can be found in Sheng *et al* (2010). CH3D uses the Reynolds-averaged Navier–Stokes (RANS) equations to compute water elevation and current velocities. To represent the vegetation-induced drag forces to the mean flow, extra profile drag $D_P$ and skin-friction drag $D_S$ are included in the RANS equations. The drag forces were formulated as (Lewellen and Sheng 1980):

$$D_{Pi} = C_p\left(u_j^2 + q^2\right)^{1/2} A_f u_i, \quad i = 1, 2 \tag{1}$$

$$D_{S_i} = C_f A_w q u_i, \quad i = 1, 2 \tag{2}$$

where $i = 1, 2$ refer to $x$ and $y$ coordinate, respectively, $u_i$ is the mean horizontal flow velocity component in the $i$th coordinate, $C_p$ is the profile drag coefficient, $C_f$ is the skin friction coefficient, $A_w$ is the wetted area per unit volume, $A_f$ is the frontal area per unit volume, $q$ is the square root of twice the turbulence kinetic energy. All variables in equations (1) and (2) can vary in the vertical direction, which usually has 4–16 layers. The profile drag coefficient $C_p$ is predetermined with typical values between 0.1 and 1.0, and the skin friction coefficient $C_f$ is computed from:

$$C_f = c_1\left(\frac{\nu}{q\Lambda}\right)^{1/4} \tag{3}$$

where $\nu$ is the kinematic viscosity, which equals $1.004 \times 10^{-6}\,\mathrm{m^2\,s^{-1}}$, and $c_1$ is an empirical constant set to 0.125 (Schlichting 1968), consistent with previous studies of Sheng and Zou (2017) and Lapetina and Sheng (2015). According to the experimental study of Tanino and Nepf (2008), the profile drag coefficient $C_p$ depends on the solid volume fraction occupied by the vegetation elements $\phi$, stem diameter $b_v$, and stem Reynolds number $\mathrm{Re_c} = \bar{u}b_v/\nu$ ($\mathrm{Re_c}$ is the Reynolds number for current, and $\bar{u}$ is the mean flow), and it has an inverse relation with $\mathrm{Re_c}$, up to $\mathrm{Re_c} = O\left(10^3\right)$, then converges to a constant value. Meanwhile, Sheng and Zou (2017) found that the model results did not show high sensitivity to $C_p$ in a range from 0.1 to 0.3 which are comparable to those used by den Hartog and Shaw (1975), Uchijima and Wright (1964), and those determined by Nepf (1999) for dense vegetation in a laboratory flume. Doubling the $C_p$ values resulted in negligible changes in the simulated inundation, hence no attempt was made to implement more complex forms of $C_p$ which vary with stem density and Reynolds number based on vegetation length scale (see e.g. Mazda *et al* 1997, Nepf and Vivoni 2000, Wamsley *et al* 2010, Nepf 2012, Hu *et al* 2015). Marsh breakage was not considered for simplicity.

In the vegetation-resolving SWAN model of Suzuki *et al* (2012), vegetation is treated as cylinder units, and the plant-induced forces (drag and inertia forces) are modeled using the formula of Mendez and Losada (2004) to account for irregular waves and depth-varying bottom, i.e. a vertical layer schematization for representing vegetation structure and calculating the dissipation term in the spectral action balance equation as:

$$\varepsilon_V = \frac{1}{2\sqrt{\pi}}\rho C_D b_v N_v \left(\frac{kg}{2\sigma}\right)^3 \frac{\sinh^3 k\alpha_v h + 3\sinh k\alpha_v h}{3k\cosh^3 kh} H_{rms}^3 \tag{4}$$

where $\rho$ is the water density, $C_D$ is the bulk drag coefficient, $N_v$ is the stem density, $k$ is the wave number, $\sigma$ is the angular frequency, $\alpha_v$ is the submergence ratio (vegetation height over water depth), $h$ is the water depth, and $H_{rms}$ refers to the root-mean-square wave height. For irregular waves, $\sigma$ and $k$ are associated with the peak wave period. Ozeren *et al* (2014) found

that the inertial force is much less significant compared with the drag force for the Keulegan–Carpenter number (KC) greater than 10, thus the ignorance of inertial force is a reasonable assumption for this study in which the KC's of all simulated cases are much greater than 10.

A theoretical expression for the wave dissipation length $L_D$ when the root-mean-square wave height at the marsh edge $H_{rms,0}$ is reduced by a ratio $\alpha$ was derived. Assuming rigid vegetation and linear wave theory in shallow waters:

$$L_D = \frac{2}{A_0 H_{rms,0}} \left( \frac{1}{\alpha} - 1 \right) \tag{5}$$

$$A_0 = \frac{C_D b_v N_v}{2h}. \tag{6}$$

Just like the turbulent eddy coefficient, drag coefficient $C_D$ has no exact solution and has to be determined empirically. We considered eight empirical formulas for $C_D$ based on mostly laboratory studies with artificial and live vegetation (Kobayashi *et al* 1993, Mendez and Losada 2004, Jadhav 2012, Koftis *et al* 2013, Anderson and Smith 2014, Möller *et al* 2014, Ozeren *et al* 2014) and one field study (Garzon *et al* 2019). A summary of these empirical formulas is presented in table SI 1. The proposed empirical relations have different definitions for Re and KC, depending on the corresponding definitions of $u_c$. Although the experiments used to fit the ensemble of empirical formulas included vegetation with stiffness from flexible to rigid and spatial scale from laboratory flume to the field, each formula is limited to certain vegetation types and hydrodynamic regimes.

Before applying CH3D-SWAN to the Piermont, we conducted simulations of two laboratory experiments, one involving flow in and around vegetation (Zong and Nepf 2010), and another involving breaking wave over a vegetated sloping bed (Wu *et al* 2011), to validate the accuracy of the model and to determine the sensitivity of model results to drag coefficients. Moreover, the model was applied to simulate wave dissipation data measured by Garzon *et al* (2019) in the Chesapeake Bay region. Results of these simulations agreed very well with measured data and are presented in the supplementary information.

## 3. Simulation of surge, wave, and flow in Piermont Marsh and Village

### 3.1. Study site

Piermont Marsh, one of four main tidal wetlands under the management of Hudson River National Estuarine Research Reserve (HRNERR), is located 40 km north of NYC, immediately south of the Village of Piermont. It is a relatively narrow marsh (approximately 1.15 km$^2$) bounded by the Hudson River with 3.2 km shoreline to the east and the uplands Tallman Mountain State Park to the west. The width of the Marsh starts from 100 m at the southern tip and increases to 600 m at the northern end. *Phragmites* dominates expansive swaths of the Marsh, including the entire margin of the Marsh abutting the Hudson River, as well as a complex network of tidal creeks.

The Marsh is a semidiurnal microtidal system with 1.21 m tidal range, and the average elevation of marshland is around 0.8 m, higher than the mean higher high water (0.63 m) (United States Geological Survey [USGSa]). Therefore, the peak high tides are usually below the marsh platform, even for spring tide conditions. With meteorological forcing, water from the Hudson River can flood the marsh platform irregularly. However, due to climate change, the coastal area around NYC is experiencing accelerated SLR with approximately twice the global rate (Horton *et al* 2015). The effect of SLR on the Marsh is not addressed here for simplicity but will be addressed in a future article.

### 3.2. Vegetation mapping and measurement

As shown in the vegetation map (figure 2(a)), Piermont Marsh is a typical example where *Phragmites* monocultures have overtaken previously biologically diverse brackish marsh plant communities (Mills *et al* 1996). In 2014, the area of *Phragmites* marsh in Piermont increased to 0.94 km$^2$, about 92% of the total marsh area.

Natural resource managers in the eastern US, including those at HRNERR and New York State Department of Environmental Conservation (NYSDEC), are concerned about the reduction of local biodiversity and productivity by the prolific *Phragmites* (Chambers *et al* 1999). Restoration efforts that replace *Phragmites* marshes with native species have often been suggested by marsh managers; for example, the restoration of native *Typha* has been proposed and is underway in three other HRNERR tidal wetlands, i.e. Tivoli Bays, Stockport Flats, and Iona Island Marsh.

Besides biodiversity-conservation considerations, the coastal protection functions of marshes, including those in the HRNERR, are also receiving more attention, especially with accelerating SLR and intensification of storms in the future. Vegetation characteristics, e.g. diameter, density, height, morphological structure, and mechanical properties, play significant roles in the vegetation–flow interactions and affect energy dissipation as well as flow pattern (Tempest *et al* 2015), which may change landscape morphology over the long term. *Phragmites* stems are considerably taller and stiffer and possess a larger diameter than previously dominant native plants, such as *Typha*, in the region (Bellavance and Brisson 2010). The sediment accretion rate in *Phragmites* marshes also tends to be higher than in those with native species, such as *Spartina alterniflora* (New Jersey Department of Environmental Protection (NJDEP)

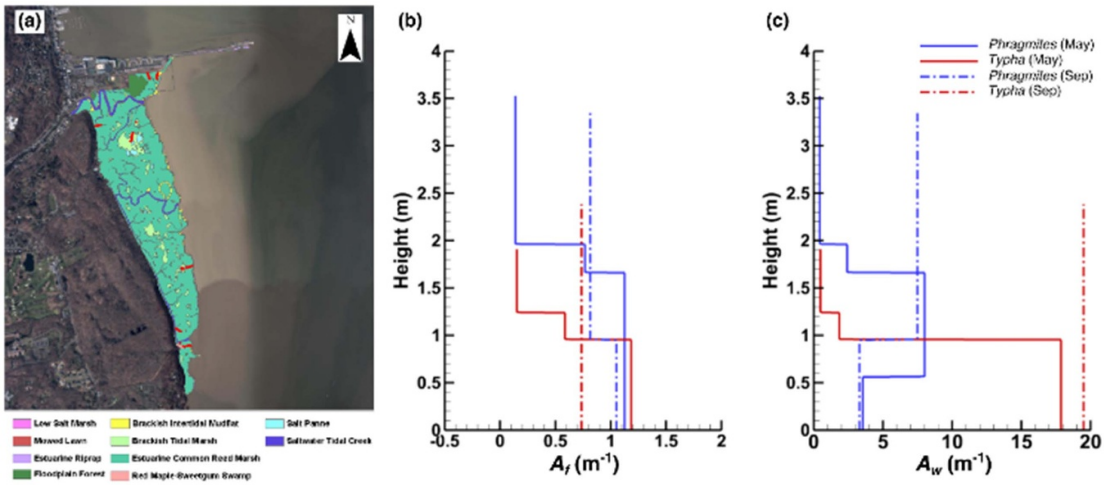


**Figure 2.** (a) Map of ecological communities in the Piermont Marsh Reserve (provided by NYSDEC) is based on a 2014 orthoimage using NY Natural Heritage Program Community Classification, and the surveyed transects (red solid lines); vertical layered structures of (b) the frontal area per volume ($A_f$) and (c) the wetted area per volume ($A_w$) for *Phragmites australis* in the Piermont Marsh and *Typha* spp. in the Iona Island Marsh surveyed in May and September of 2017. Map reproduced from Piermont Marsh Storm Protection Study (2020). Image stated to be in the public domain.

2020). Therefore, it is necessary to develop a better understanding of Marsh's unique capability to attenuate storm-induced flood and wave damage on residential structures before carrying out any restoration project.

Two field surveys were conducted in May (late spring) and September (early fall) 2017 to measure the vegetation structure in both seasons in the study area. The height, diameter, stem density, and leaves were measured along transects (red solid lines in figure 2(a)) for *Phragmites* and native species (*Scirpus* spp. and *Spartina patens*) in the Piermont Marsh. The same data were collected for *Typha* in the nearby Iona Island Marsh (18 miles north of the Piermont Marsh). The vertically varying frontal area per volume $A_f$ and the wetted area per volume $A_w$ were then calculated (figures 2(b) and (c)) from measured stem density and diameter and leaf area following Lapetina and Sheng (2014). A *Typha* plant is characterized by long strap-like leaf blades branching out from shoot base; whereas the leaf blades of a *Phragmites* plant are relatively shorter and grow between the middle and upper levels of the stem. Denser leaf blades of *Typha* greatly increase the wetted area compared with *Phragmites*. In May, canopies are mixed with short young, broken, and unbroken dead stems, resulting in multiple layered morphological structures—and this vertical variation of stem density is more pronounced for *Typha*—whereas the morphology is relatively uniform in September as live plants are fully grown. The frontal areas of *Phragmites* and *Typha* at the bottom layer in late spring are greater than those in early fall due to the existence of broken plant stems (left from last growing season) and the seasonal emergence of short new shoots. Phragmites produce more litter on the surface, and this litter decays more slowly, and therefore traps more sediment for a longer time.

### 3.3. Model setup

#### *3.3.1. Hydrodynamic model setup*

A high-resolution curvilinear grid, nested within a regional-scale domain (figure 1(a)), was developed for the Piermont area, nearby uplands, as well as the surrounding tidal river (Hudson River) and creek system (figure 1(c)). The grid had an average cell size of 6.45 m, the minimum cell size reached 0.62 m in the tidal creeks, and the resolution of land cells was 1–3 m, sufficient to resolve the flow in the main tidal creeks and overland flooding. Hudson River bathymetry collected by NYSDEC with 1 m resolution in 2014–2015 was used. For shallow waters and land area that the dataset did not cover, a seamless bathymetry and topography dataset (1/9 arc-sec resolution) from Hurricane Sandy Digital Elevation Models (National Center for Environmental Information) was used. All the vertical positions were referenced to the NAVD88.

This study examined the impacts of the Piermont Marsh on flooding, waves, currents, and structural losses during Sandy. The open boundary conditions along the southern and northern boundaries were extracted from a large-scale domain Sandy simulation. As shown in figure 3(a), the peak water levels at the boundary cells lied in between the surveyed high-water marks at NYROC07562 (USGSb) and NYWES07662 (USGSc), indicating high confidence of the boundary conditions for the fine-scale simulations. Winds (figure 3(b)) recorded at the Hudson River Environmental Conditions Observing System weather station at Piermont Pier were used to provide the meteorological forcing. Before Sandy's landfall, the study area experienced north-easterly wind. As the eye of Sandy approached NJ shore, wind in Piermont gradually increased to 19.65 m s$^{-1}$ and switched clockwise to easterly-south-easterly. In the

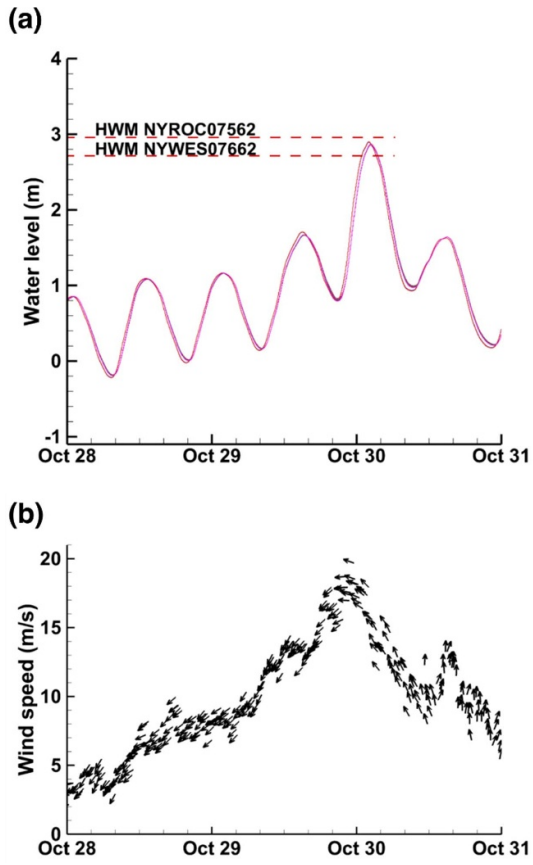


**Figure 3.** (a) Time series of water elevation specified as open boundary conditions on the southern and northern boundary cells. The water elevation data were computed from the large-scale domain simulation; (b) time series of recorded wind speed (m $s^{-1}$) and direction at Piermont Pier during Sandy (data from Hudson River Environmental Conditions Observing System).

meantime, as the peak storm tide reached Piermont from NYC, it was 9.5 ft (2.9 m).

*3.3.2. Input for vegetation module*

Due to high Re ($O(10^3)$) during storm conditions, the profile drag coefficient $C_p$ is in the convergence region. As in Sheng and Zou (2017), a series of $C_p$ values (0.1–0.3) were tested, with negligible difference for the flooding results. Therefore, $C_p$ was set to 0.2 to account for the lower modulus of elasticity of marsh vegetation compared with rigid cylinders.

For simulating wave dissipation by vegetation, we calculated the values of $C_D$ using the empirical formulas discussed earlier and the vegetation and wave orbital velocity data of Piermont Marsh. We chose to use a value of 0.86, about half of the value given by Ozeren *et al* (2014), for Piermont Marsh due to the good performance of Ozeren *et al* (2014) for the laboratory experiments and the more flexible nature of *Phragmites* stems compared to the Birch dowel used by Chapman *et al* (2015). Unless indicated explicitly, the vegetation characteristics surveyed in September 2017 and $C_D$ of 0.86 were used in the model. Sensitivity analysis showed that the increased drag coefficient would slightly reduce the dissipation distance without changing the results at Piermont Village.

Multiple-layered $A_f$ and $A_w$ shown in figure 2 were input to the model to represent the *Phragmites* and *Typha* marshes, and a uniform morphological structure with a density of 600 stems $m^{-2}$, stem diameter of 3.5 mm, and height of 0.9 m, was used to compute $A_f$ and $A_w$ for the small native marsh patches where *Scirpus* and *S. patens* were dominant. In comparison, Piermont Marsh had a stem density of ∼100 stems $m^{-2}$, stem diameter of ∼0.5 cm, and a height of 3.38 m.

## 4. Simulation results

To understand the role of Piermont Marsh in reducing damage to the Village of Piermont during Sandy, we simulated the flooding, currents, and wave in the Piermont Marsh and Village area. The results are summarized below.

### 4.1. Simulated inundation during Sandy

As shown in figures 4(a) and (b), inundation in the Village was barely reduced (<2 cm) by the Marsh, due to its relatively narrow width (∼500 m) along the mostly Easterly peak wind direction. The results were similar if the Marsh were replaced by *Typha*, as shown in figure 4(c). During Sandy, the simulated maximum water level was 2.88 m at a house in the southern Village and 2.86 m at the Village Pier (figure 4(d)), within 3% of the observed values. If the Marsh were removed, the corresponding values would become 2.89 m and 2.86 m. The residential properties of the Village are shown in figure 4(f).

### 4.2. Simulated currents during Sandy

As shown in figure 5, surface currents in the southern Village would be very strong if the Marsh were removed, while the existing Marsh as well as a 0917 (September 2017) *Typha* Marsh both significantly reduced the surface currents from 60 cm $s^{-1}$ (current speed before the water interacted with the marsh) to less than 5 cm $s^{-1}$, which would minimize the transport of debris from outside the southern edge of the Marsh into the Village. With the 0517 (May 2017) Marsh structure, the existing *Phragmites* Marsh would significantly reduce the currents, while the *Typha* Marsh with considerably shorter and sparser plant canopy would not.

### 4.3. Simulated wave height

As shown in figure 6, without the Marsh, the significant wave height at the southern Village would have been more than 50 cm, barely dissipated from the wave height at the edge of the Marsh of about 60 cm. With the existing Marsh or a 0917 *Typha* Marsh, wave height was significantly dissipated to about 15–20 cm. Within about 150 m, the wave height was dissipated by more than 50%, consistent with the dissipation

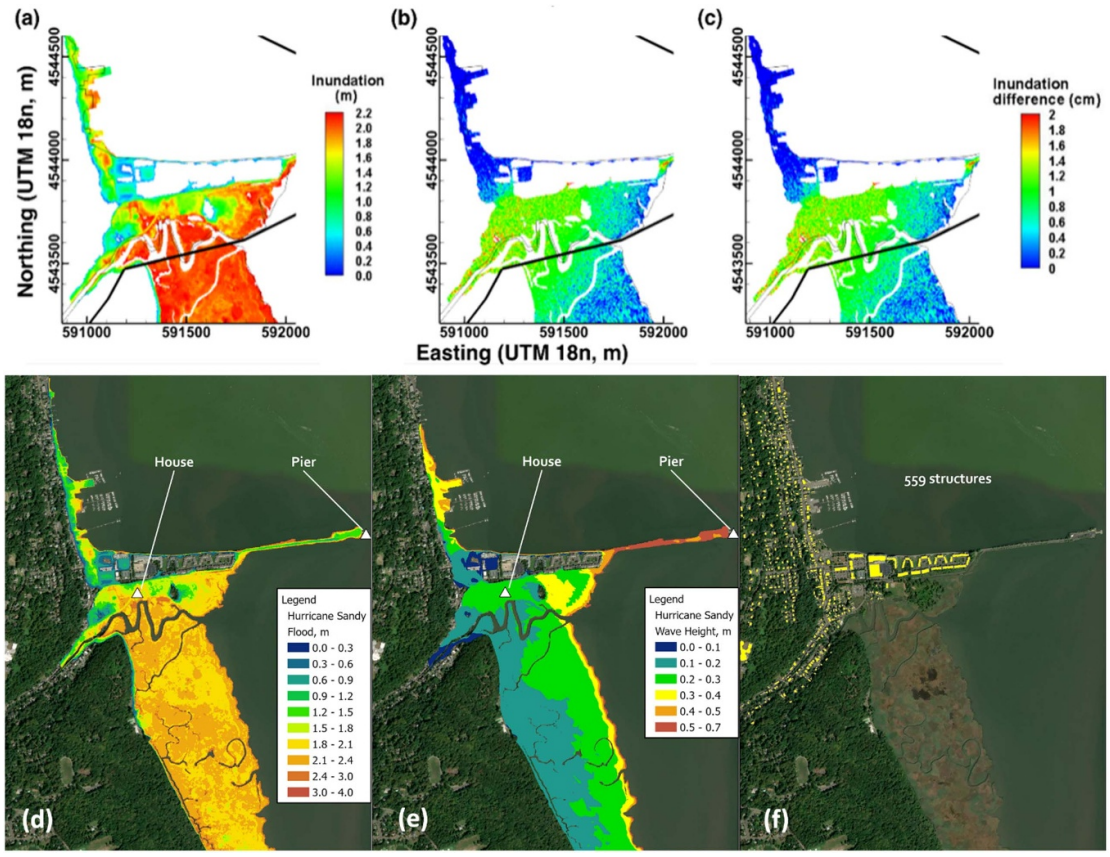


**Figure 4.** (a) Maximum inundation during Sandy with Marsh removed; (b) reduction in maximum inundation by the existing Marsh; (c) reduction in maximum inundation by a *Typha*-based Marsh; (d) maximum inundation during Sandy with existing Marsh; (e) maximum significant wave height during Sandy with existing Marsh; (f) residential properties map.

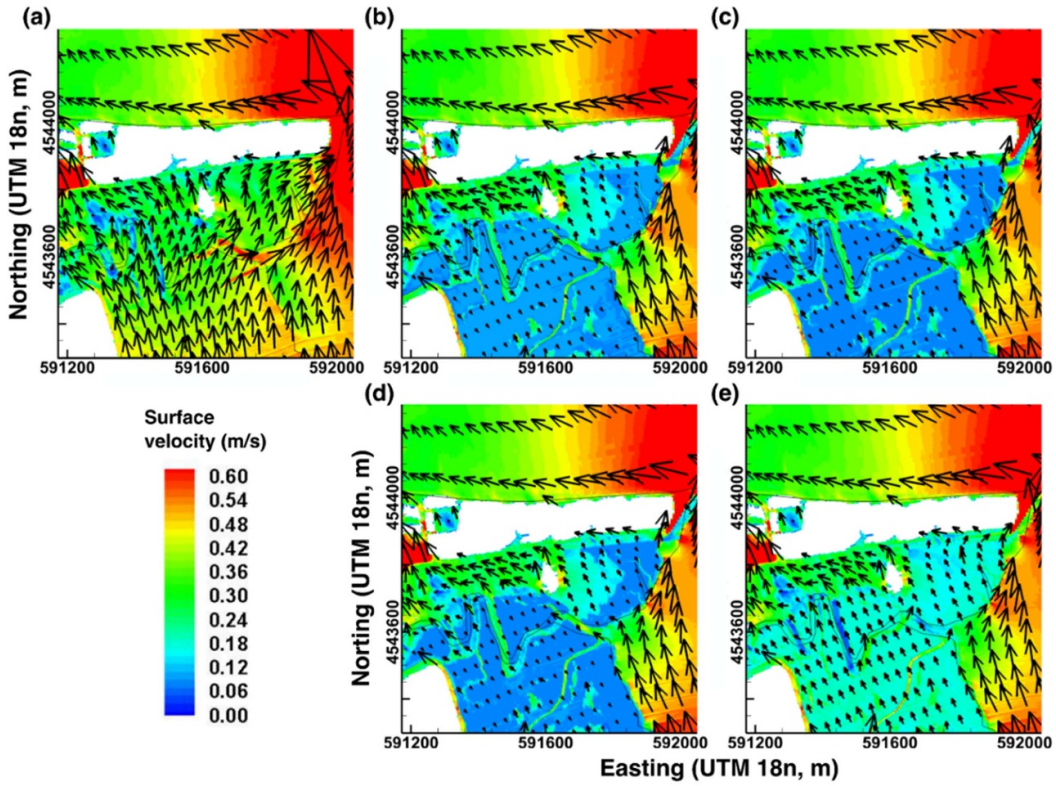


**Figure 5.** Surface-layer currents in the southern area of the Piermont Village at 0230 UTC 30 October from the simulations with (a) no vegetation, (b) the original marsh in September, (c) the restored marsh in September, (d) the original marsh in May, and (e) the restored marsh in May.

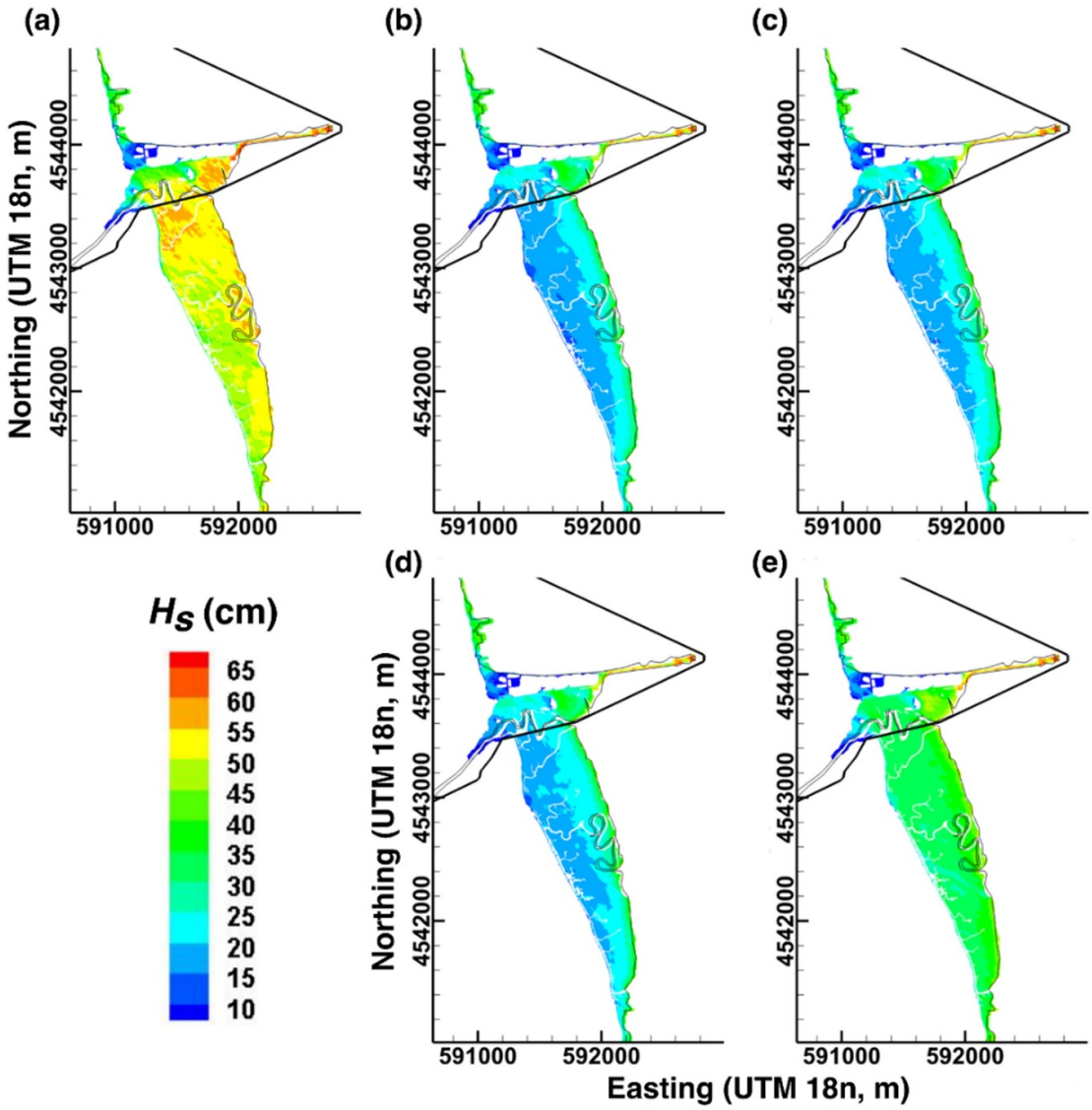


**Figure 6.** Spatial distributions of maximum significant wave height from the simulations with (a) no vegetation, (b) the existing *Phragmites* marsh in September, (c) the *Typha* Marsh in September, (d) the existing Marsh in May, and (e) the *Typha* Marsh in May.

length shown in equation (5). With the 0517 Marsh structure, the existing *Phragmites* Marsh would still significantly reduce the wave height while the seasonally lower *Typha* Marsh would not.

## 5. Economic analysis of the role of Piermont Marsh during Sandy

As a first step to assess the ecosystem service value of the Piermont Marsh in reducing property damage due to flood and wave during storms, we conducted a parcel-based economic analysis using the simulated inundation and wave along with the best available building footprint data (NYS GIS Clearinghouse) and damage functions from the U.S. Army Corps of Engineers (U.S. Army Corps of Engineers (USACE) 2015). The height of the wave crest (WC) curve was used in regions where the depth limited controlling wave height $H_C$ was greater than 1.5 ft, while flood depth curve was used elsewhere. Here, WC is defined as:

$$\mathrm{WC} = 0.7 \times H_c + d \tag{7}$$

where $d$ is the still water elevation. Our estimated property damage of \$3.72 M for the 41 properties that received \$3.56 M NFIP payouts had an error of 4.4%. The actual claims might have been greater than the payouts because many claimers were either uninsured or under-paid. Table 1 shows that flood and wave accounted for ~70% and ~30% of the structural loss. If all the 500+ buildings in the Village were included in the damage analysis, the estimated loss of \$11.9 M (with 71% being flood damage) is less than the total estimated loss of \$20 M (including losses that were not included in our analysis) by the Village of Piermont (2014), with an avoided loss of \$902 K

**Table 1.** Simulated flood loss, wave loss, and total loss for the with and without Piermont marsh scenarios during Sandy and for the 1% annual chance flood and wave.

| Cause of structural loss | Structural loss | Superstorm Sandy | Ensemble of storms (1% annual event) |
|---|---|---|---|
| Flood | With marsh | $8 495 493 | $11 128 825 |
| | Without marsh | $8 497 893 | $12 330 743 |
| | Avoided loss | $2400 | $1 201 918 |
| | Relative avoided loss (% of with-marsh loss) | 0.03% | 10.80% |
| Wave | With marsh | $3 436 302 | $7 691 374 |
| | Without marsh | $4 335 763 | $8 623 170 |
| | Avoided loss | $899 462 | $931 796 |
| | Relative avoided loss (% of with-marsh loss) | 26.18% | 12.11% |
| Total | With marsh | $11 931 795 | $18 820 199 |
| | Without marsh | $12 833 656 | $20 953 913 |
| | Avoided loss | $901 862 | $2 133 714 |
| | Relative avoided loss (% of with-marsh loss) | 7.56% | 11.34% |

(7.6% of the actual loss). The relative wave loss was 26.2%.

Sheng *et al* (2012) found that surge dissipation varies significantly with local wetland type, cross-shore wetland width, and storm characteristics. While the Marsh was not effective in reducing flood damage during Sandy, it could significantly buffer flood damage during a different storm with different intensity and wind direction. Therefore, to calculate the value of Piermont Marsh in reducing structural loss, it is necessary to consider an ensemble of storms with lesser intensity but higher frequencies. To this end, we used the joint probability method with optimal sampling JPM-OS (Condon and Sheng 2012, Yang *et al* 2019) to generate a set of optimal storms to represent all possible storms predicted by the North Atlantic Stochastic Hurricane Model NASHM (Hall and Jewson 2007, Hall and Yonekura 2013). Following Yang *et al* (2019), we calculated the 1% annual chance flood and wave maps for Piermont and the associated structural loss due to flood and wave. Table 1 shows that the estimated structural loss for the 1% annual chance event was $18.82 M where wave accounted for ∼60% of the loss. The relative avoided loss due to flood and wave was 11.34% and 12.1%, respectively.

## 6. Conclusions

A comprehensive study was conducted to examine the role of the *Phragmites*-dominated Piermont Marsh in buffering wave and flood-induced structural loss in the Village of Piermont during Sandy. The study used a vegetation-resolving three-dimensional surge-wave modeling system CH3D-SSMS with 0.62–6.45 m resolution, with detailed marsh data and forcing conditions provided by simulated and observed wind and water level data at the air–sea interface and the model open boundary, respectively. Before application to Piermont, the model was used successfully to simulate two laboratory experiments, one on flow in vegetation and one on wave dissipation over a sloping beach, plus one field measurement in the Chesapeake Bay. Appropriate drag coefficients were determined.

Our results showed that during Sandy, the high wave energy in the Hudson River was significantly (56%) dissipated by the *Phragmites*-dominated Piermont Marsh before reaching the Piermont Village. On the other hand, only 1% of the flood was dissipated by the relatively narrow marsh width subject to peak easterly wind. The Marsh was able to significantly reduce the current and prevent the river-borne debris from transporting across the Marsh and reaching the Village. If the tall and rigid *Phragmites* were replaced by the slightly shorter *Typha* found in nearby Iona Marsh, the wave and debris buffering capacity of the Marsh would have been preserved during Sandy when both plants were tall and dense in the fall. However, if the Marsh were replaced by *Typha* and experienced a Sandy-like storm during the non-growth season (e.g. May), the Marsh's buffering capacity would be greatly reduced relative to the existing Marsh. The shorter and sparser *Typha* marsh would not have provided much buffering during the frequent N'easters in winter and spring.

Using the simulated flood and wave over the Piermont Village with residential property data and damage functions, our estimate of structural loss due to flood and wave during Sandy was $11.93 M, compared to the more than $20 M losses including rebuilding and income losses reported by Village of Piermont. If the Piermont Marsh were absent, the total loss would have increased by 8% to $12.83 M due to 26% increase in wave-induced damage. The estimated losses for the 1% annual chance event at Piermont Village are $18.82 M and without the Marsh, they could reach $20.95 M. Thus, Piermont Marsh is preventing $21 300 in annualized loss. While the

avoided losses during Sandy were mainly associated with wave-induced damage, the avoided losses of the 1% annual chance event were a combination of flood (11%) and wave (12%) induced losses. Since the 1% annual chance flood is generated by storm events that are more frequent but less intense than Sandy, our results are consistent with the claims by Rezaie *et al* (2020) that wetlands are more efficient in buffering more frequent storms with lower intensities relative to less frequent, but more energetic events like Superstorm Sandy.

Our comprehensive study confirmed that the value of marsh for flood protection depends significantly on vegetation type, storm characteristics, and local community. The 200+ acre tall (>2 m) and dense Piermont marsh is found to provide significant protection for Piermont Village during storms. If the marsh were made of short (<1 m) and sparse *Spartina* along New Jersey coast, they would not have been able to protect the Village from Sandy, consistent with the finding of Lathrop *et al* (2019) for South Jersey. Importantly, extensive model verification with available data (vegetation, water level, wave, and structural loss) during Sandy confirmed the robustness of our study. However, although detailed vegetation data was used, we did not include the damage of vegetation due to excessive wind or hydrodynamic loading. The damage assessment used actual building data but relied on empirical damage functions. To reduce uncertainties in the future, species-dependent storm-induced vegetation damage can be investigated, and more robust building-specific damage functions can be developed. Nevertheless, our study provided realistic assessment on the value of the Piermont Marsh for flood protection, which can be used as guideline for resilience and restoration planning by the Village and marsh managers. This study demonstrated the significant value of the invasive common reed, *Phragmites*, in protecting coastal communities from storm-induced structural loss. Moreover, Rooth and Stevenson (2000) and New Jersey Department of Environmental Protection (NJDEP) (2020) found that *Phragmites* enables marshes to elevate faster than native species. Therefore, natural resource managers considering eradicating *Phragmites* to enhance biodiversity and other ecosystem functions should weigh the tremendous value of *Phragmites* in protecting coastal communities from structural damage due to storms and SLR to develop site-specific restoration plans that balance biodiversity and coastal resilience. The role of Piermont Marsh in protecting Piermont Village from future flood and wave damage will be examined in an upcoming paper.

## Data availability statement

The data that support the findings of this study are available upon reasonable request from the authors.

## Acknowledgments

This work was sponsored by the National Estuarine Research Reserve System Science Collaborative, which supports collaborative research that addresses coastal management problems important to the reserves. The Science Collaborative is funded by the National Oceanic and Atmospheric Administration and managed by the University of Michigan Water Center (NAI4NOS4190145) with Lynn Vaccaro as the project manager. We also appreciate the support from the NOAA Climate Program Office Grant No. NA11OAR4310105. HRNERR (Sarah Fernald, Heather Gierloff, and Betsy Blair) provided the original Piermont Marsh distribution data and valuable support for field research. Timothy Hall at NASA-GISS provided the NASHM storm ensemble for the tri-state region. Klaus Jacob provided logistic support for water level and wave measurement. Bennett Brooks, Emilie Hauser, Sarah Fernald, Heather Gierloff, Nathan Mitchell, and Klaus Jacob provided valuable assistance in communicating the scientific results to the community and resource manager. There is no conflict of interest for all authors.

## ORCID iD

Y Peter Sheng https://orcid.org/0000-0001-8827-1451

## References

Anderson M E and Smith J M 2014 Wave attenuation by flexible, idealized salt marsh vegetation *Coast. Eng.* **83** 82–92

Bellavance M E and Brisson J 2010 Spatial dynamics and morphological plasticity of common reed (*Phragmites australis*) and cattails (*Typha* sp.) in freshwater marshes and roadside ditches *Aquat. Bot.* **93** 129–34

Benoit L K and Askins R A 1999 Impact of the spread of *Phragmites* on the distribution of birds in Connecticut tidal marshes *Wetlands* **19** 194–208

Blake E S, Kimberlain T B, Berg R J, Cangialosi J P and Beven II J L 2013 Tropical Cyclone Report Hurricane Sandy (AL182012) (22–29 October 2012) National Oceanic and Atmospheric Administration—National Hurricane Center

Booij N, Ris R C and Holthuijsen L H 1999 A third-generation wave model for coastal regions: 1. Model description and validation *J. Geophys. Res. Oceans* **104** 7649–66

Chambers R M, Meyerson L A and Saltonstall K 1999 Expansion of *Phragmites australis* into tidal wetlands of North America *Aquat. Bot.* **64** 261–73

Chapman J A, Wilson B N and Gulliver J S 2015 Drag force parameters of rigid and flexible vegetal elements *Water Resour. Res.* **51** 3292–302

Condon A J and Sheng Y P 2012 Optimal storm generation for evaluation of the storm surge inundation threat *Ocean Eng.* **43** 13–22

den Hartog G and Shaw R H 1975 A field study of atmospheric exchange processes with a vegetative canopy *Heat and Mass Transfer in the Biosphere* ed D A DeVries and N H Afgan (Trenton, NJ: Scripta Book Company) pp 299–309

Federal Emergency Management Agency (FEMA) 2013 Hurricane Sandy in New Jersey and New York: building performance

observations, recommendations, and technical guidance *Mitig. Assess. Team Rep.* p 223
Garzon J L, Maza M, Ferreira C M, Lara J L and Losada I J 2019 Wave attenuation by *Spartina* saltmarshes in the Chesapeake Bay under storm surge conditions *J. Geophys. Res. Oceans* **124** 5220–43
Hall T M and Jewson S 2007 Statistical modelling of North Atlantic tropical cyclone tracks *Tellus* A **59A** 486–98
Hall T and Yonekura E 2013 North American tropical cyclone landfall and SST: a statistical model study *J. Clim.* **26** 8422–39
Hanson S R, Osgood D T, Yozzo D J and Vittor B A 2002 *Nekton Use of a Phragmites australis Marsh on the Hudson River, New York, USA* vol 22 (Berlin: Springer)
Horton R, Bader D, Kushnir Y, Little C, Blake R and Rosenzweig C 2015 New York City panel on climate change 2015 ReportChapter 1: climate observations and projections *Ann. N. Y. Acad. Sci.* **1336** 18–35
Hu K, Chen Q and Wang H 2015 A numerical study of vegetation impact on reducing storm surge by wetlands in a semi-enclosed estuary *Coast. Eng.* **95** 66–76
Hu Z, Suzuki T, Zitman T, Uittewaal W and Stive M 2014 Laboratory study on wave dissipation by vegetation in combined current-wave flow *Coast. Eng.* **88** 131–42
Hudson River Environmental Conditions Observing System (HRECOS) Historical Data (available at: https://hrecos.org/index.php?option=com_content&view=article&id=143&Itemid=54)
Jadhav R 2012 Field investigation of wave and surge attenuation in salt marsh vegetation and wave climate in a Shallow Estuary LSU Dr Diss. (available at: https://digitalcommons.lsu.edu/gradschool_dissertations/3939)
Kettenring K M and Adams C R 2011 Lessons learned from invasive plant control experiments: a systematic review and meta-analysis *J. Appl. Ecol.* **48** 970–9
Kettenring K M, McCormick M K, Baron H M and Whigham D F 2011 Mechanisms of *Phragmites australis* invasion: feedbacks among genetic diversity, nutrients, and sexual reproduction *J. Appl. Ecol.* **48** 1305–13
Kiviat E 2013 Ecosystem services of *Phragmites* in North America with emphasis on habitat functions *AoB Plants* **5**
Kobayashi N, Raichle A W and Asano T 1993 Wave attenuation by vegetation *J. Waterway Port Coast. Ocean Eng.* **119** 30–48
Koftis T, Prinos P and Stratigaki V 2013 Wave damping over artificial *Posidonia oceanica* meadow: a large-scale experimental study *Coast. Eng.* **73** 71–83
Lal R 2004 Soil carbon sequestration impacts on global climate change and food security *Science* **304** 1623–7
Lapetina A and Sheng Y P 2014 Three-dimensional modeling of storm surge and inundation including the effects of coastal vegetation *Estuar. Coasts* **37** 1028–40
Lapetina A and Sheng Y P 2015 Simulating complex storm surge dynamics: three-dimensionality, vegetation effect, and onshore sediment transport *J. Geophys. Res. Oceans* **120** 7363–80
Lathrop R G, Irving W, Seneca J J, Trimble J and Sacatelli R M 2019 The limited role salt marshes may have in buffering extreme storm surge events: case study on the New Jersey shore *Ocean Coast. Manage.* **178**
Lewellen W S and Sheng Y P 1980 Modeling of dry deposition of $SO_2$ and sulfate aerosols *Final Report* (available at: www.osti.gov/servlets/purl/5278148/)
Losada I J *et al* 2018 The global value of mangroves for risk reduction *Technical Report* 42
Mazda Y, Magi M, Kogo M and Hong P N 1997 Mangroves as a coastal protection from waves in the Tong King Delta, Vietnam *Mangroves Salt Marshes* **1** 127–35
Mendez F J and Losada I J 2004 An empirical model to estimate the propagation of random breaking and nonbreaking waves over vegetation fields *Coast. Eng.* **51** 103–18
Mills E L, Strayer D L, Scheuerell M D and Carlton J T 1996 Exotic species in the Hudson River basin: a history of invasions and introductions *Estuaries* **19** 814–23
Möller I *et al* 2014 Wave attenuation over coastal salt marshes under storm surge conditions *Nat. Geosci.* **7** 727–31
Narayan S, Beck M W, Wilson P, Thomas C J, Guerrero A, Shepard C C, Reguero B G, Franco G, Ingram J C and Trespalacios D 2017 The value of coastal wetlands for flood damage reduction in the Northeastern USA *Sci. Rep.* **7** 9463
National Center for Environmental Information Hurricane Sandy digital elevation models (available at: www.ngdc.noaa.gov/mgg/inundation/sandy/sandy_geoc.html)
Nepf H M 1999 Drag, turbulence, and diffusion in flow through emergent vegetation *Water Resour. Res.* **35** 479–89
Nepf H M 2012 Flow and transport in regions with aquatic vegetation *Annu. Rev. Fluid Mech.* **44** 123–42
Nepf H M and Vivoni E R 2000 Flow structure in depth-limited, vegetated flow *J. Geophys. Res. Oceans* **105** 28547–57
New Jersey Department of Environmental Protection (NJDEP) 2020 *The Status and Future of Tidal Marshes in New Jersey Faced with Sea Level Rise* (Trenton, NJ)
NYS GIS Clearinghouse NYS GIS Program Office New York State tax parcels (available at: http://gis.ny.gov/gisdata/inventories/details.cfm?DSID=1300)
Ozeren Y, Wren D G and Wu W 2014 Experimental investigation of wave attenuation through model and live vegetation *J. Waterway Port Coast. Ocean Eng.* **140** 04014019
Paramygin V A, Sheng Y P and Davis J 2017 Towards the development of an operational forecast system for the Florida coast *J. Mar. Sci. Eng.* **5** 8
Rezaie A M, Loerzel J and Ferreira C M 2020 Valuing natural habitats for enhancing coastal resilience: wetlands reduce property damage from storm surge and sea level rise *PLoS One* **15**
Rooth J E and Stevenson J C 2000 Sediment deposition patterns in *Phragmites australis* communities: implications for coastal areas threatened by rising sea-level *Wetl. Ecol. Manage.* **8** 173–83
Schlichting H 1968 *Boundary Layer Theory:* 6th edn McGraw-Hill Series in Mechanical Engineering (New York: McGraw-Hill) pp 747
Sheng Y P 1986 A three-dimensional mathematical model of coastal, estuarine and lake currents using boundary-fitted grid *Technical Report* 585 (Princeton, NJ: Aeronautical Research Associates of Princeton, Inc.)
Sheng Y P 1989 Evolution of a three-dimensional curvilinear-grid hydrodynamic model for estuaries, lakes and coastal waters: CH3D *Proc. 1st Int. Conf. on Estuarine and Coastal Modeling, American Society of Civil Engineers* pp 40–9
Sheng Y P, Alymov V and Paramygin V A 2010 Simulation of storm surge, wave, currents, and inundation in the Outer Banks and Chesapeake bay during Hurricane Isabel in 2003: the importance of waves *J. Geophys. Res. Oceans* **115** C04008
Sheng Y P, Lapetina A and Ma G 2012 The reduction of storm surge by vegetation canopies: three-dimensional simulations *Geophys. Res. Lett.* **39** 2012GL053577
Sheng Y P, Rivera-Nieves A, Zou R and Paramygin V 2021 Role of wetlands in reducing structural loss is highly dependent on characteristics of storms and local wetland and structure conditions *Nat. Sci. Rep.* **11** 5237
Sheng Y P and Zou R 2017 Assessing the role of mangrove forest in reducing coastal inundation during major hurricanes *Hydrobiologia* **803** 87–103
Suzuki T, Zijlema M, Burger B, Meijer M C and Narayan S 2012 Wave dissipation by vegetation with layer schematization in SWAN *Coast. Eng.* **59** 64–71
Tanino Y and Nepf H M 2008 Laboratory investigation of mean drag in a random array of rigid, emergent cylinders *J. Hydraul. Eng.* **134** 34–41
Tempest J A, Harvey G L and Spencer K L 2015 Modified sediments and subsurface hydrology in natural and

recreated salt marshes and implications for delivery of ecosystem services *Hydrol. Process.* **29** 2346–57

Theuerkauf S J, Puckett B J, Theuerkauf K W, Theuerkauf E J and Eggleston D B 2017 Density-dependent role of an invasive marsh grass, *Phragmites australis*, on ecosystem service provision, ed J Liu *PLoS One* **12** e0173007

Toyama T, Nishimura Y, Ogata Y, Sei K, Mori K and Ike M 2016 Effects of planting *Phragmites australis* on nitrogen removal, microbial nitrogen cycling, and abundance of ammonia-oxidizing and denitrifying microorganisms in sediments *Environmental Technology (United Kingdom)* vol 37 (Taylor and Francis) pp 478–85 (available at: https://pubmed.ncbi.nlm.nih.gov/26198662/)

U.S. Army Corps of Engineers (USACE) 2015 Physical depth damage function summary report, North Atlantic comprehensive coastal study: resilient adaptation to increasing risk (available at: www.nad.usace.army.mil/Portals/40/docs/NACCS/10A_PhysicalDepthDmgFxSummary_26Jan2015.pdf)

Uchijima Z and Wright J L 1964 An experimental study of air flow in a corn plant-air layer *Bull. Natl Inst. Agric. Sci. Japan* **A11** 19–65

United States Geological Survey (USGSa) Current conditions for USGS 01376269 Hudson River at Piermont NY (available at: https://waterdata.usgs.gov/ny/nwis/uv?site_no=01376269)

United States Geological Survey (USGSb) Short-term network monitoring (NYROC07562) (available at: https://stn.wim.usgs.gov/STNPublicInfo/#/HWMPage?Site=7562&HWM=6425)

United States Geological Survey (USGSc) Short-term network monitoring (NYWES07662) (available at: https://stn.wim.usgs.gov/STNPublicInfo/#/HWMPage?Site=7662&HWM=6549)

Village of Piermont 2014 *Resilience Roadmap: Planning for Piermont's Future, Report of the Piermont Waterfront Resilience Task Force* (Piermont Village, NY)

Wamsley T V, Cialone M A, Smith J M, Atkinson J H and Rosati J D 2010 The potential of wetlands in reducing storm surge *Ocean Eng.* **37** 59–68

Weinstein M P and Balletto J H 1999 Does the common reed, *Phragmites australis*, affect essential fish habitat? *Estuaries* **22** 793–802

Weinstein M P, Litvin S Y, Bosley K L, Fuller C M and Wainright S C 2000 The role of tidal salt marsh as an energy source for marine transient and resident finfishes: a stable isotope approach *Trans. Am. Fish. Soc.* **129** 797–810

Weis J S 2005 Diet and food web support of the white perch, *Morone americana*, in the Hackensack Meadowlands of New Jersey *Environ. Biol. Fishes* **74** 109–13

Weis J S and Weis P 2003 Is the invasion of the common reed, *Phragmites australis*, into tidal marshes of the eastern US an ecological disaster? *Mar. Pollut. Bull.* **46** 816–20

Windham L, Weis J S and Weis P 2001 Lead uptake, distribution, and effects in two dominant salt marsh macrophytes, *Spartina alterniflora* (cordgrass) and *Phragmites australis* (common reed) *Mar. Pollut. Bull.* **42** 811–6

Wu W *et al* 2011 Phase I Report for SERRI Project No. 80037: investigation of surge and wave reduction by vegetation (Oak Ridge, TN)

Yang K, Paramygin V A and Sheng Y P 2019 An objective and efficient method for estimating probabilistic coastal inundation hazards *Nat. Hazards* **99** 1105–30

Zong L and Nepf H 2010 Flow and deposition in and around a finite patch of vegetation *Geomorphology* **116** 363–72